A novel sensor based on nanobiocomposite AuIn_2O_3 chitosan modified acetylene black paste electrode for sensitive detection of antimycoticciclopirox olamine

Hossieny Ibrahim, Yassien Temerk, Nasser Farhan

www.elsevier.com/locate/talanta

PII: S0039-9140(17)31076-7
DOI: https://doi.org/10.1016/j.talanta.2017.10.036
Reference: TAL18034

To appear in: *Talanta*

Received date: 8 August 2017
Revised date: 18 October 2017
Accepted date: 20 October 2017

Cite this article as: Hossieny Ibrahim, Yassien Temerk and Nasser Farhan, A novel sensor based on nanobiocomposite AuIn_2O_3 chitosan modified acetylene black paste electrode for sensitive detection of antimycoticciclopirox olamine, *Talanta,* https://doi.org/10.1016/j.talanta.2017.10.036

A novel sensor based on nanobiocomposite Au-In_2O_3 -chitosan modified acetylene black paste electrode for sensitive detection of antimycotic ciclopirox olamine

Hossieny Ibrahim*, Yassien Temerk* and Nasser Farhan

Chemistry Department, Faculty of Science, Assiut University, Assiut, Egypt

ABSTRACT

For the first time, a sensitive conductive nanobiocomposite sensor consisting of Au–In_2O_3 nanocomposite and chitosan (CS) was successfully prepared and used for the modification of acetylene black paste electrode (Au-In_2O_3-CS/ABPE). The phase structures, composition and morphology of Au–In_2O_3 nanocomposite were characterized by X-ray diffraction (XRD), energy–dispersed X-ray (EDX) and transmission electron microscopy (TEM). Electrochemical activities and surface analysis of the biosensor electrode Au-In_2O_3-CS/ABPE were investigated using scanning electron microscopy (SEM), cyclic voltammetry and square wave voltammetry. The modified electrode showed an excellent electrochemical activity toward the electro–oxidation of the antimycotic ciclopirox olamine (CPX) leading to a significant improvement in sensitivity as compared to the bare ABPE. The proposed biosensor demonstrated linearity in the range 0.199 – 16.22 μmol L^{-1}, with high sensitivity (64.57 μA μmol L^{-1} cm^{-2}) and detection limit of 6.64×10^{-9} mol L^{-1} CPX. The analytical performance of this biosensor was evaluated for detection of CPX in pharmaceutical formulations with good accuracy and precision. This proposed method was validated by UPLC and the results are in agreement at the 95% confidence level.

Keywords: Au loaded In_2O_3, Nanobiocomposite, Batrafen cream, Ciclopirox olamine, Chitosan

*Corresponding author: Tel.: +20 (88) 2080770; fax: +20 (88) 2080209

E-mail addresses:

Hossienyomer@yahoo.com, hossieny.ibrahim@aun.edu.eg (H. Ibrahim)

Temerk44@yahoo.com, temerk@aun.edu.eg (Y.Temerk)

1. Introduction

In recent years, nanocomposite materials have been interestingly studied for electrochemical sensing applications. Some special properties can be considered in modification of the electrodes using nanomaterials, e.g., catalysis, the large specific surface area and more adsorption sites [1, 2]. In particular oxide nanocomposites have been used in numerous fields of application, biosensors, gas sensors, conductive paints, drug delivery and rechargeable batteries [3, 4] due to the novel properties of nanocomposite which can be derived from the successful blending of the characteristics of the parent constituents into a single material. Among metal oxide, indium oxide (In_2O_3) is an important semiconductor with a wide direct band gap (3.55eV–3.75eV) and high conductivity [5, 6]. Due to its unique catalytic, optical electronic and gas sensing properties, In_2O_3 can be used as a catalyst, luminophors, electrodes, solar cells and gas sensors [7]. Additionally, the nanostructured In_2O_3 often exhibits shape and size dependent physical and chemical properties, which are of importance and interest to specific research [8]. Interestingly, the surface modification of In_2O_3 with noble metal such as Au is considered as effective strategies to improve its structural properties for various applications. In our work, Au nanoparticles were loaded on the In_2O_3 surface; they enrich the conversion of oxygen species and the reaction rate between oxygen species and target molecule, which can ultimately improve the sensing properties. In addition, the presence of AuNPs could significantly enhance the photoelectric properties of In_2O_3 nanoparticles. Hence, this study investigates the application of the Au loaded In_2O_3 that have entrapped in the large surface area of chitosan for fabrication of a highly sensitive and stable electrochemical nanobiocomposite sensor. Such an interest in CS has arisen from its excellent biocompatibility, biodegradability, nontoxicity, high mechanical strength, cheapness and susceptibility to chemical modifications [9, 10]. Hence, in this work a novel ternary nanobiocomposite Au-In_2O_3-CS modified acetylene black paste electrode (Au-In_2O_3-CS/ABPE) was constructed and applied for selective and sensitive determination of the antimycotic CPX in pharmaceutical formulations without physiological interferents. To the best of our knowledge, no previous report in the literature was described for detecting the CPX by electrochemical methods using nanobiocomposite electrodes.

Ciclopirox (6-cyclohexyl-1-hydroxy-4-methyl-2(1H)- pyridone) (Scheme1) is a substituted antimycotic pyridone, widely used as an antifungal substance in pharmaceutical preparations as well as an antiseborrheic agent in cosmetics [11]. Ciclopirox olamine (CPX) also displays promising

anticancer activity in preclinical models of several cancers [12-14]. For example, it was found that CPX inhibits the growth and viability of acute myeloid leukemia cell lines and primary patient samples in vitro and in vivo, including the leukemic stem cell fraction [14]. The wide spread use of this compound and the need for clinical and pharmaceutical study require fast and sensitive analytical techniques to assay the presence of this drug in pharmaceutical dosage forms and also in biological samples. In scientific literature, there are not many methods for the quantitative determination of CXP. The USP has published two standard methods in pharmaceutical formulations, thought HPLC [15] and spectrophotometry [16, 17]. Others methods applied to biological and pharmaceutical samples consider the use of liquid chromatography [18], micro-liquid chromatography [11], spectrofluorimetry [19], amperometry [20, 21], polarography [22, 23], voltammetry [24] micellar electrokinetic capillary chromatography [25], liquid chromatography quadrupole mass spectrometry [26], capillary electrophoresis [27] and thermal lens spectrophotometry [28]. Most of these methods have their own short comings, such as time-consuming, low sensitivity and complicate experimental process. As a comparison, electrochemical analysis demonstrates its outstanding merits in terms of instrumentation costs, operation convenience and on-site rapid application [29]. It is worth stressing that electrochemical methods using the modified electrodes have attracted large interest due to their potential applications in various analysis [30-32]. However, using nanobiocomposite Au-In_2O_3-CS into the acetylene black paste as a novel electrochemical sensor for sensitive detection of CPX has never explored until now.

The objective of the present work is to combine the excellent electrocatalytic and synergistic properties of AuNPs decorated In_2O_3 with the large surface area of porous chitosan for the fabrication of modified acetylene black paste electrode. The fabricated nanobiocomposite Au-In_2O_3-CS/ABPE exhibited good performance along with high sensitivity, excellent selectivity and fast SWV response for the detection antimycotic CPX. The modified electrode was successfully applied for assay of CPX in pharmaceutical formulations, such as Batrafen cream and Batrafen ear drops with satisfactory results, which is due to its high surface area, abundant active sites and the catalysis of AuNPs. Consequently, the proposed sensor is a promising application in biosensing.

Scheme1 Here

2. Experimental

2.1. Reagents and solutions

Ciclopirox olamine, chloroauric acid and indium(III) nitrate hydrate were purchased from Sigma-Aldrich chemicals (St. Louis, Mo, USA). Acetylene black and paraffin oil were obtained from Alfa Aesar (Ward Hill, MA). A stock solution of CPX was prepared by dissolving an appropriate amount of the compound in ethanol and storing the solution in the dark at 4 °C. Britton-Robinson (BR), acetate (AB) citrate (CB), phosphate (PB) and McIlvaine (MB) buffers were used as supporting electrolytes. The pH of the aqueous solutions was measured using a pH-meter (Model 3310 pH-meter Jenway) with accurate to ±0.02 unit. All of the chemicals were of reagent grade, (Merck, Darmstadt). High-quality deionized water was obtained by passing distilled water through a Milli-Q plus System (Millipore, Merck). Deinoized water was used to prepare all the solutions.

2.2. Apparatus

Cyclic voltammetry (CV) and square-wave voltammetry (SWV) were performed using an EG&G PAR 384 B (Princeton Applied Research, Oak Ridge, TN, USA) polarographic analyzer controlled by 394 software in conjunction with a PAR Model 303A. The electrode system consisted of the acetylene black paste electrode (unmodified or modified) as the working electrode, a Ag/AgCl (saturated KCl) reference electrode and a Pt wire auxiliary electrode. A PAR Model 305 stirrer was used for SWV. For anodic stripping experiments an accumulation potential (E_{acc}) was applied for a certain accumulation time (t_a), while the solution was stirred at 400 rev/min. At the end of the accumulation period the stirrer was stopped and the solution was allowed to become quiescent for 15s prior of the voltammetric scan. The chromatography was performed on an ACQUITY ultra performance liquid chromatography (UPLC) system (Waters Corp., Model code CHA, Singapore). The UPLC system included quaternary solvent manager, a binary pump, degasser, auto sampler with an injection loop of 10 µL and a column heater-cooler. The separation was performed on Acquity UPLC BEH C18 column (50 × 2.1 mm, i.d., 1.7 µm, Waters, Ireland) maintained at 30 °C. The mobile phase was composed of acetonitrile: water (50:50 v/v) at a flow rate of 0.4 mL min^{-1}, detection was monitored at 305 nm, and chromatographic run time of 10.0 min. The injection volume was 1.0 µL. Chromatographic data was acquired using Empower 2 software. The surface morphology of the samples is analyzed by transmission electron microscopy, TEM (FEI, TECNAI, G2 spirit twin) using

an accelerating voltage of 120 KV. Specimens for TEM are prepared by ultrasonic dispersion of some powder sample in ethanol and putting a droplet of the suspension on a copper microscope grid covered with carbon.

2.3. Preparation of In_2O_3NPs and Au-In_2O_3 nanocomposite

In_2O_3NPs and Au-In_2O_3 nanocomposite were synthesized by hydrothermal method. In this method 4 mmol $In(NO_3)_3 \cdot 4.5H_2O$ and 4 g urea were dissolved in 50 ml of diethylene glycol (DEG), stirring for 3 h to form a homogeneous solution. Then transferred the mixed solution into a 100 mL Teflon-lined stainless steel autoclave and maintained the temperature at 140 ºC for 24 h. After the autoclave cooled to room temperature naturally, the as-prepared precipitates were collected by centrifugation and washed several times by deionized water and absolute ethanol and dried at 60 ºC for 12 h. The obtained sample was annealed in a muffle furnace at 500 ºC for 2 h in air to form In_2O_3NPs. Next, 200 mg as-obtained In_2O_3 product and 1.0 mL of 0.01 mol L^{-1} chloroauric acid solution were dispersed into 50 mL deionized water by ultrasonication for 30 min, the obtained slurry was transferred to a Teflon-lined stainless steel autoclave and heated at 140 ºC for 10 h. Finally, the product was dried at 60 ºC for 10 h to obtain the final product of Au-In_2O_3 nanocomposite.

2.4. Preparation of ABPE and Au-In_2O_3-CS/ABPE

Acetylene black paste electrode (ABPE) was prepared by mixing AB (60 wt%) with a binder (paraffin oil) (40 wt%) and the blend was mixed until a homogenous paste with the appropriate consistence was obtained. The paste was packed firmly into the cavity of a Teflon tube (3 mm diameter) to a depth of 6mm, and an electrical contact was achieved via a copper wire. The electrode surface was smoothed against weighing paper. It is important to note that the amount of paraffin oil must be carefully controlled because excessive paraffin oil will lower the conductivity of AB paste, while insufficient paraffin oil is not beneficial to obtain uniform AB paste. The bionanocomposite Au-In_2O_3-CS modified ABPE was prepared by mixing AB (50 wt%), Au-In_2O_3 (10 wt%), 100 µL chitosan (0.5 mg mL^{-1} chitosan (CS) solution was prepared by dissolving CS in 1 % acetic acid solution with

magnetic stirring for 3 h) and paraffin oil (40 wt%). The surface of Au-In_2O_3-CS/ABPE was polished on a piece of weighing paper to get a smooth surface just before use.

2.5. Determination of CPX in pharmaceutical preparations

A weighed quantity of the Batrafen cream equivalent to 10 mg of the drug was transferred into a small beaker, extracted with 50 ml of ethanol into 100 ml measuring flask. The solution was completed to the volume with the same solvent. This solution was centrifuged for 20 min at 4000 rpm. The clear supernatant layer was filtered through 0.45 µm milipore. Appropriate aliquot of this solution was diluted with supporting electrolyte to a predefined concentration.

A 20 µL of Batrafen solution (ear drops) was added to 5 mL of MB of pH 4.0. For SWV measurements, the test solution was placed in a polarographic cell. The standard addition method was then applied, adding successive concentrations of CPX. In this context, further spiking with standard concentrations of CPX into the fresh sample yielded a systematic increase in the peak currents over the respective potential, evidence that the peak current corresponds to the presence of CPX in the real sample.

3. Results and discussion

3.1. Phase structures, composition and morphology of In_2O_3NPs and Au-In_2O_3 nanocomposite

In order to determine the phase composition crystal structure of pure In_2O_3 nanoparticles and Au-In_2O_3 nanocomposite, we employed X-ray diffractometer. Figure 1 shows the XRD patterns of pure In_2O_3 and Au-In_2O_3 nanocomposite. As we can see from the XRD patterns of In_2O_3NPs, all the main peaks can be accurately indexed to the cubic structure of In_2O_3 (JCPDS card No. 04-014-4391) and no impure peaks are detected. The average particle size is estimated to be ~17-21 nm according to the Debye-Scherrer's equation [33]. As for the XRD pattern of Au-In_2O_3 nanocomposite, it can be obviously observed that the position of main peaks is same to that of In_2O_3 samples. We can also observed that besides the diffraction peaks of In_2O_3, the XRD pattern of Au-In_2O_3 also shows four small peaks compared with pure In_2O_3 samples, which can be ascribed to the (111), (200) (220) and (311) planes of face-centered cubic (fcc) Au (JCPDS No. 01-071-4614). The selected-area electron

diffraction (SAED) pattern (inset of Fig. 1) clearly displays diffraction rings indexed as (211), (222), (400), (440) and (622) planes of cubic In_2O_3, in accordance with the XRD characterization and indicating the polycrystalline nature of In_2O_3NPs.

Figure1 Here

EDX analysis is carried out to determine the chemical composition of the Au-In_2O_3 nanocomposite (Fig. S1). From the spectrum we can know that there are three elements in this sample: Au, In, O. The weight percent of Au is 2.93 wt%, which is approach to the theoretical value (3 wt%).

In order to obtain more detailed information about the internal nanostructure and morphology of the In_2O_3NPs and Au-In_2O_3 nanocomposite, the TEM analysis was employed. Figure 2(a) shows the TEM image of In_2O_3 nanocube with the diameter of about 20 nm. Figure 2(b&c) shows the TEM images of the Au-In_2O_3 nanocomposite. The Au nanoparticles can be observed. Figure 2(d) exhibits the high-resolution (HRTEM) image of lattice fringes of Au and In_2O_3. The spacing of lattice fringes of Au is measured to be about 0.231 nm. It can be assigned to the (111) crystal planes of Au. The spacing of lattice fringes of In_2O_3 is about 0.291 nm and it can be assigned to the (222) crystal planes of cubic In_2O_3.

Figure2 Here

3.2. Surface morphology of the biosensor Au-In_2O_3-CS/ABPE

The morphologies of bare ABPE, In_2O_3/ABPE, Au-In_2O_3/ABPE and Au-In_2O_3-CS/ABPE were studied using SEM. Significant differences in the surface structure of four electrodes were observed. The SEM profile of ABPE displayed a spherical morphology (Fig.3a). Despite the presence of the mineral oil, AB nanoparticles were packed in close proximity, and no defined binder regions were visible. Apparently, only a little amount of mineral oil filled the voids between the AB holding them together. The SEM of In_2O_3/ABPE showed that a mass of In_2O_3 nanoparticles is filled in the gaps among the nanospheres (Fig.3b). In Fig. 3(c) shows Au-In_2O_3 nanocomposite present as clusters along AB nanoparticles. The SEM image of Au-In_2O_3-CS/ABPE shows that the surface was smooth and glazed, indicating that CS exhibits good adherence of Au-In_2O_3 to AB nanoparticles (Fig. 3d). Moreover, Au-In_2O_3-CS/ABPE possesses a large surface area, numerous active sites and good electric conductivity

Figure3 Here

3.3. Characterization of the Au-In_2O_3-CS/ABPE

The $[Fe(CN)_6]^{3-/4-}$ redox probe is used for the electrode characterization and the electrochemical response from Fe^{3+}/Fe^{2+} redox couple can reflect the conductivity of the electrode interface. The electrochemical behaviour of the bare ABPE, CS/ABPE, In_2O_3/ABPE, Au-In_2O_3/ABPE and Au-In_2O_3-CS/ABPE was investigated using $[Fe(CN)_6]^{3-/4-}$ as a redox probe. Figure 4 shows the cyclic voltammograms of 5 mmol L^{-1} $[Fe(CN)_6]^{3-/4-}$ containing 0.1 mol L^{-1} KCl in potential range of -0.4 V to 1.10 V at given electrodes. Figure 4(a) is a cyclic voltammogram curve of bare ABPE, which has a pair of redox peaks with the anodic peak potential (E_{pa}) as 450 mV and the cathodic peak potential (E_{pc}) as 84 mV. The anodic peak current (I_{pa}) and the cathodic peak current (I_{pc}) are got as 50 μA and 60 μA, respectively. The Peak-to-peak potential separation (ΔE_P) is 366 mV and the ratio of I_{pa} / I_{pc} is 0.83. The results indicated that the electrode reaction was a quasireversible process. Figure 4(b) is a cyclic voltammogram curve of CS/ ABPE with E_{pa} of 472 mV, E_{pc} of 88 mV and ΔE_P of 384 mV. Figure 4(c) is a cyclic voltammogram curve of In_2O_3/ABPE with E_{pa} of 402 mV, E_{pc} of 84 mV and ΔE_P of 318 mV. Figure 4(d) is a cyclic voltammogram curve of nanocomposite Au-In_2O_3 incorporated ABPEs with E_{pa} of 364 mV, E_{pc} of 128 mV and ΔE_P of 263 mV. The voltammetric response was dramatically improved at the nanobiocomposite Au-In_2O_3-CS modified ABPE. The obtained results indicated an increase in the current response at different electrodes and the increase order was: I_P (bare ABPE) < I_P (CS/ABPE) < I_P (In_2O_3/ABPE) < I_P (Au-In_2O_3/ABPE) < I_P (Au-In_2O_3-CS/ABPE). Meanwhile, a decrease in the peak-to-peak separation (ΔE_P) was observed and the decrease order was: ΔE_P (Au-In_2O_3-CS/ABPE) < ΔE_P (Au-In_2O_3/ABPE) < ΔE_P (In_2O_3/ABPE) < ΔE_P (CS/ABPE) < ΔE_P (ABPE). These observations suggested that nanobiocomposite Au-In_2O_3-CS could greatly promote the electron transfer of $[Fe(CN)_6]^{3-/4-}$.

Figure4 Here

Figures S2&S3 show various CVs recorded at different scan rates (50–500 mVs^{-1}) for ABPE and Au-In_2O_3-CS/ABPE in 0.1 mol L^{-1} KCl containing 5 mmol L^{-1} of $[Fe(CN)_6]^{3-/4-}$. It can be seen that the anodic potential shifts towards positive side and the cathodic peak potential shifts in the reverse

direction. Besides this, the redox peak currents are proportional to the square root of scan rate which indicates diffusion electron-transfer process.

The active surface area of the unmodified and modified electrode was estimated according to the slope I_P versus $\nu^{½}$ for a known concentration of $[Fe(CN)_6]^{3-/4-}$ based on Randles–Sevcik equation [34]

$$I_p = 2.69x10^5\, n^{3/2}\, A\, D^{1/2}\, \nu\, C \quad (1)$$

Where n is the value of electron transfer (n=1), A is the active electrode area, D is the diffusion coefficient ($7.6x10^{-6}$ cms^{-1}), C is the concentration of $[Fe(CN)_6]^{3-/4-}$ (5mmol L^{-1}) and ν is the scan rate. By exploring the redox peak current with scan rate, the average electroactive area of unmodified ABPE and modified Au-In_2O_3-CS/ABPE was calculated as 0.17 cm^2 and 0.48 cm^2, respectively. The result further indicated the presence of nanobiocomposite Au-In_2O_3-CS greatly improved the effective area of the electrode surface, which led to the great enhancement of electrochemical response on the modified electrode.

3.4. Electrocatalytic oxidation of CPX at Au-In_2O_3-CS/ABPE

To investigate the electrocatalytic activity toward of CPX, the bare ABPE, CS/ABPE, In_2O_3/ABPE, Au-In_2O_3/ABPE and nanobiocomposite Au-In_2O_3-CS modified ABPE were characterized by CV over the range of 0.6 V to 1.2 V in McIlvaine buffer (MB) of pH 4.0 at scan rate 100 mVs^{-1}. As shown in Fig. 5(a) only one oxidation peak was observed showing that CPX underwent an irreversible redox process. The oxidation of CPX at ABPE occurred at the potential of 0.917 V with poor current response (I_p = 1.70 μA) (curve 1), indicating a slow electron transfer kinetics, which might ascribed to low electrical conductivity and low surface area of the electrode. Compared to those obtained at the bare ABPE (curve1), CS/ABPE (curve2), In_2O_3/ABPE (curve3), Au-In_2O_3/ABPE (curve4) and Au-In_2O_3-CS/ABPE (curve5) a remarkably large peak current was observed at nanobiocomposite Au-In_2O_3-CS/ABPE. This anodic peak current obtained for nanobiocomposite Au-In_2O_3-CS modified electrode nearly 3.5 fold higher when compared to bare electrode. Modification of ABPE with Au-In_2O_3-CS not only enhanced the oxidation current but also reduced the over potential for electrooxidation of CPX. The remarkable enhancement of current response demonstrated that nanobiocomposite Au-In_2O_3-CS acted as an efficient promoter to improve the electron transfer kinetics. Meanwhile, the highest peak current of CPX observed at Au-In_2O_3-CS/ABPE indicated that the

synergistic effect of nanocomposite Au-In_2O_3 and CS was present on the electrode surface. Due to the co-contribution of Au-In_2O_3 and CS, the modified electrode acted as a very efficient promoter to enhance the electrochemical kinetics for CPX and the electrochemical responses were greatly enhanced, which provided a platform for sensitive determination of CPX.

Figure5 Here

The electrochemical behaviour on bare, CS/ABPE, In_2O_3/ABPE, Au-In_2O_3/ABPE and Au-In_2O_3-CS modified ABPE was also investigated via SWV. From the distinctive difference of the oxidation peak between curves in Fig. 5(b), it could be inferred that the catalysis toward CPX oxidation at Au-In_2O_3-CS/ABPE was ascribed to the nanobiocomposite Au-In_2O_3-CS. The oxidation peak at the Au-In_2O_3-CS/ABPE was larger than that on bare ABPE (14.8 fold greater). It implies that the co-existence of CS with the Au-In_2O_3 enhances the electrochemical performance of the sensor. The enhancement of current response is a clear indication of the electrocatalytic activity of Au-In_2O_3-CS/ABPE sensor toward the oxidation of CPX. This can be attributed to the presence of Au-In_2O_3-CS, which promoted the electron transfer and endows electrocatalysis toward CPX at this Au-In_2O_3-CS modified sensor as a result of its specific properties, such as high electrical conductivity and high specific area (Scheme2). It is clear that the increase in oxidation current at the proposed electrode can provide a new avenue for electrochemical determination of CPX in different pharmaceutical dosage forms.

Scheme2 Here

3.5. Effect of nano-Au-In_2O_3

Since, it was expected that the amount of nano-Au-In_2O_3 in the modified electrode exerts a significant on the anodic adsorptive stripping of CPX, seven modified electrodes of ABPE containing different quantities of nano-Au-In_2O_3 were constructed, while the concentration of CS was fixed at 100µL (0.5 mg ml^{-1}). As shown in Fig. 6 for chemically modified ABPE with 0.0 to 15 wt% nano-Au-In_2O_3, the resulting current level corresponding to CPX oxidation increases with the percentage of nano-Au-In_2O_3 up to 10 wt% and levels off at higher concentrations. This because the sites for catalysis increased with the increase of nano-Au-In_2O_3 percentage in the modified electrode, while the excess of nano-Au-In_2O_3 decreased the efficient area of the electrode. The relation between the percentage of

nano-Au-In_2O_3 in the ABPE and the anodic oxidation peak current of CPX indicated also the electrochemical oxidation of CPX is more facile on 10wt% nano-Au-In_2O_3. The results confirmed the key role played by nano-Au-In_2O_3 on the catalytic oxidation of CPX which enhances the electrochemical reaction. In addition, Au additives can promote In_2O_3 to form active sites on their surface which is considered to be an important reason for the enhanced response of CPX compared with unmodified ABPE.

Figure6 Here

3.6. Effect of CS

In order to optimize the response to CPX, Au-In_2O_3-CS/ABPEs were prepared containing different concentrations of CS (0.5mg ml^{-1}) loading from 0.0 to 200 μL, while the percentage of Au-In_2O_3 nanocomposite was fixed at 10 wt%. The dependence of the sensitivity of CS loading is shown in Fig. 7. It can be clearly seen that the sensitivity of the modified electrode improved as the amount of CS was increased up to 100 μL, when the highest response was obtained. The results demonstrated that the presence of CS in the acetylene black paste electrode could improve both the sensitivity and repeatability of the modified electrode. Increasing CS loading above this concentration decreased the sensitivity, probably because of steric hinderance of CS and due to the reduction of the conductive area of the electrode surface. Hence, the electrode composition of 10wt% nano-Au-In_2O_3, 60 wt% AB, 100 μL CS and 30 wt% paraffin oil was employed for all subsequent experiments.

Figure7 Here

3.7. Effect of supporting electrolyte and pH

The electrochemical behaviour of 4.03 μmol L^{-1} CPX at Au-In_2O_3-CS/ABPE was investigated in various buffer solution systems such as Britton-Robinson, McIlvaine, acetate, phosphate and citrate buffers. It was found that the CV peak relatively high sensitivity and better shape could be obtained in McIlvaine buffer solutions (Fig. S4). Considering the sensitivity and well defined peak of CPX, McIlvaine was chosen as the optimized supporting electrolyte, in which the electron conductivity ability of Au-In_2O_3 could be activated. Therefore, McIlvaine buffer was used throughout in the following experiments. To further understand the electrochemical performance of CPX at the surface of

Au-In_2O_3-CS/ABPE modified electrode, the effect of pH on the peak potential and current of CPX was investigated. As can be seen in Fig. S5 the oxidation peak current of CPX increases with increasing pH value until it reaches 4.0 and then decreases with increasing pH value further. This is due to the presence of amine group within chitosan structure, which is protonated in acid medium, hence attracting the nucleophilic regions of CPX and favoring its oxidation. Considering, the sensitivity for determining CPX, pH 4.0 is chosen for the subsequent analytical experiments. Meanwhile, with pH value of the solution increasing, the oxidation peak potential (E_{pa}) shifts negatively, indicating that protons have taken part in the electrode reaction of CPX. A good linear relationship was observed between E_{pa} and pH value in the range of 3–8 (Fig. 8). This relationship can be described by the following equation: $E_p(V) = 1.01 - 0.056$ pH ($R^2 = 0.9899$). The slope of the linear equation is 0.056 $mVpH^{-1}$ which closes to the Nernstian value of 0.059 $mVpH^{-1}$ at 25 ºC. This result revealed that the number of protons in the process is equal with the number of electrons transfer in the oxidation reaction of CPX.

Figure8 Here

3.8. Effect of scan rate on the oxidation of CPX at Au-In_2O_3-CS/ABPE

The kinetics of the electrode reaction was investigated by studying effect of scan rate on the anodic peak current of CPX (Fig. 9a). Scan rate studies were carried out to assess whether the processes on Au-In_2O_3-CS/ABPE were under diffusion or adsorption control. As shown in Fig. 9(b), the anodic peak current (I_{pa}) of CPX increased with increasing scan rate on Au-In_2O_3-CS/ABPE in McIlvaine buffer of pH 4.0 and exhibited a linear relation to square root of the scan rate, $\nu^{1/2}$, with the linear regression equation $I_{pa}(\mu A) = 0.17 + 0.39\ \nu^{1/2}$ (mVs^{-1}) (R = 0.996). The result indicates that the electron transfer reaction is controlled by the diffusion of CPX. The effect of scan rate on the peak current was also examined under the above conditions with a plot of logarithm of anodic peak current (Log I_{pa}) *versus* logarithm of scan rate (Log ν), giving a straight line within the same range with a slope of 0.504 (Fig. 9c) closes to the theoretical value of 0.5, which is expected for an ideal reaction for diffusion-control electrode process [35]. This linear relationship was obtained as follows: log I_P (μA) = 0.504 logν (mVs^{-1}) – 0.41 (R = 0.9976).

Figure9 Here

Moreover, the peak potential shifted to more positive values on increasing the same scan rate, which confirms the irreversibility of the oxidation process of CPX. The plot of E_P *versus* log ν was linear; having a correlation coefficient of 0.9996 and the relation between peak potential and log ν can be expressed as: E_P (V) = 0.056 logν (Vs^{-1}) + 0.92.

According to the Laviron theory for irreversible electrode process [36], E_P is defined by the following equation.

$$E_P = E^o - (2.3RT/\alpha nF) [\log (RTk_s / \alpha nF) - \log \nu] \qquad (2)$$

Where α is the transfer coefficient, k_s is the heterogeneous electron transfer rate constant, n is the number of electrons transferred, ν is the scan rate, and E^o is the formal redox potential. Other symbols have their common meanings. Thus value of αn can be easily calculated from the slope of E_P vs. log ν (Fig. S6). In this system, the slope was found to be 0.056 taking T = 298 K, R = 8.314 J/K mol, and F = 96480 C/mol, the αn was calculated to be 1.047. The value of α can be calculated as:

$$E_P - E_{P/2} = (47.7/\alpha)\ mV \qquad (3)$$

Where $E_{P/2}$ is the potential when the current is at half the peak value. From this, we obtained the value of α to be 0.52 for Au-In_2O_3-CS/ABPE. So, the number of electrons (n) transferred in the electrooxidation of CPX was calculated to be 2.01≈ 2.

The value of k_s can be determined from the intercept of the previous plot if the values of αn and E^o are known. The value of E^o can be obtained from the intercept of E_P *versus* ν curve by extrapolating to the vertical axis at ν = 0 Vs^{-1}. Thus, using this information and Eq. (2) the k_s values obtained were 0.42×10^2 and 11.52×10^2 s^{-1} for bare and modified electrodes, respectively. The obtained results may be attributed to the good electrical conductivity as well as the increase of the electrode surface area in the presence of nanobiocomposite Au-In_2O_3-CS and suggested that electron transfer process between the CPX molecules and the modified electrode was very fast.

The surface concentration of electroactive species (Γ, mol cm^{-2}) can be calculated from the slope of the plot of I_{pa} versus scan rate by [37]: $I_p = n^2F^2\nu A\ \Gamma/4RT$ where n is the number of electrons transferred, F (C/mol) is the Faraday's constant, A (cm^2) is the area of the electrode, Γ is the surface concentration of the electroactive substance, CPX, and ν (Vs^{-1}) is the scan rate. The surface concentration (Γ) of electroactive CPX on Au-In_2O_3-CS/ABPE was calculated as 1.92×10^{-10} mol cm^{-2}, which was much higher than that on bare ABPE (5.66×10^{-11} mol cm^{-2}). The result can be attributed to

the existence of nanobiocomposite Au-In_2O_3-CS providing a large surface area and promoting the electron transfer of CPX.

3.9. Electrochemical conditions optimization

Before electrochemical measurements, optimum conditions for SWV were recognized by measuring the current dependence on instrumental parameters counting frequency (f), pulse height (ΔE_a) and scan increment (ΔE_s). Therefore, SW voltammograms of CPX in MB of pH 4.0 at the nanobiocomposite Au-In_2O_3-CS/ABPE were recorded at various parameters of the excitement signal. The variables of interest were studied over the range 5–40 mVpp of pulse height, 20–120 Hz of frequency and 2–10 mV scan increment. The better developed voltammetric peak was obtained under the following pulse parameters: f = 100 Hz, ΔE_a = 30 mVpp and ΔE_s = 8 mV using Au-In_2O_3-CS/ABPE. These parameters reflect voltammograms of high sensitivity, well-shaped wave and best peak morphology.

The effect of accumulation potential and time on the oxidation peak current of CPX was studied by SWV. When the accumulation potential (E_{acc}) was varied from -0.2 – 0.3 V vs. Ag/AgCl, the peak current increased because the applied potential is near the oxidation potential of CPX and therefore the CPX molecules tend to accumulate at the electrode surface. But at potential higher than +0.1V vs. Ag/AgCl the peak current dramatically decreased by applying the potentials that are higher or about the oxidation potential of CPX, the drug molecules do not have any time to accumulate at the surface. Therefore, the accumulation efficiency decreased and the electrochemical signals were decreasing consequently. Hence, a potential of +0.1V vs. Ag/AgCl was applied as accumulation potential.

The dependence of oxidation of CPX on the accumulation time was also studied in the presence of 4.03 µmol L^{-1} CPX. As expected the peak current of CPX increased remarkably as the accumulation time (t_{acc}) increased from 0 to 70 sec, the peak current tended to be almost stable (Fig. S7). This behaviour is consistent with a process that is limited by accumulation of reactant at the electrode surface due to the saturation of the surface [38]. Considering sensitivity and analysis time, the accumulation time of 70 s was employed.

3.10. Stability, repeatability and reproducibility of the fabricated biosensor

In order to investigate the stability of the biosensor Au-In_2O_3-CS/ABPE by CV in MB of pH4.0 containing 4.03 µmol L^{-1} CPX, continues cycles were carried out at a scan rate 100 mVs^{-1}. The results show only a 3.25 % loss after 25 cycles. When the electrode was kept in air at room temperature for 6 weeks, the peak currents retained more than 96.50% of their initial values. The excellent operational and storage stability obtained were most like due to the porosity of CS supporting material and the strength of In_2O_3 nanoparticles that helped to increase both the chemical and mechanically stability of the sensing layer decorated with AuNPs.

To characterize the reproducibility of the modified electrode, five Au-In_2O_3-CS/ABPEs were fabricated simultaneously in the same conditions. The electrode-to-electrode reproducibility was examined using SWV method for a CPX solution and was no significant change in the current response (RSD% = 2.13). To evaluate the repeatability of the Au-In_2O_3-CS/ABPE, ten measurements for each of the three concentrations of CPX covering the lower linear range, 0.4, 1.77 and 7.10 µmol L^{-1} CPX produced RSDs of 2.39, 2.15 and 1.87%, respectively. The obtained results demonstrated that modified electrode Au-In_2O_3-CS/ABPE possessed acceptable repeatability, reproducibility and excellent stability for SWV detection of the antimycotic CPX in real samples which was very important for the development of the proposed biosensor in low cost application.

3.11. Validation studies and analytical performance

After the optimal conditions were established for CPX detection, the parameters were used to plot calibration curves. SW voltammograms responses at the Au-In_2O_3-CS/ABPE toward different concentrations of CPX in MB of pH4.0 were measured in the potential range from 0.3 V to 1.1 V with frequency 100 Hz and pulse height 30 mVpp. In Fig. 10 SW voltammograms show well-defined and stable anodic oxidation peak of CPX. These demonstrated that nanobiocomposite Au-In_2O_3-CS modified electrode might provide a good electrocatalytic activity toward CPX sensing. A linear dynamic range of 0.199 µmol L^{-1} to 16.22 µmol L^{-1} CPX was obtained following its concentration onto the modified electrode by accumulation for 70 s at +0.1V (Fig. S8). A linear relationship was extracted between the anodic peak current and the CPX concentration, using the following regression equation: Ip(µA) = 4.52 CPX (µM) + 0.04 (R^2 = 0.9994). In this context the reproducible sensitivity and limit of

detection (LOD) of the proposed sensor were found to be 64.57 μA μmol L^{-1} cm^{-2} and 6.64×10^{-9} mol L^{-1}, respectively demonstrating the sensitivity of the method (Table1). These good performances indicated that the Au-In_2O_3-CS modified electrode is a powerful biosensor for the direct detection of CPX. This is most likely because of the large surface area of CS porous structure that can help increase the amount entrapped sensing materials and the accessibility of CPX solution to the electrode.

Table1 Here

The LOD of CPX was compared with the values reported by other reported analytical methods in Table2. The obtained LOD value for CPX is evidently lower as compared with the data reported previously for determination of CPX. The wide linear range and low LOD can attributed to the effect of the nanobiocomposite Au-In_2O_3-CS, which provided a large specific area to increase the loading amount of CPX on the electrode surface. Meanwhile, the electron transfer to the electrode surface can be accelerated and the electrochemical signal is amplified due to the outstanding electrical conductivity of the modifier. It can be concluded that the combined properties of a large surface area together with the enhancement of electron transfer to the sensing part led to a highly sensitive detection of CPX. The aforementioned results indicate that the proposed SWV procedure using renewable Au-In_2O_3-CS/ABPE provides a convenient and efficient method for quantification of CPX.

Figure10 Here

Table2 Here

Intra-day accuracy and precision of assay CPX utilizing Au-In_2O_3-CS/ABPE were evaluated by the analysis of 0.4, 1.77 and 7.10 μmol L^{-1} CPX in the same day. The inter-day studies were performed of seven days over one weak (after 1, 2, 4, 5 and 7 days of electrode storage). The results obtained for intra-day and inter-day precision and accuracy were presented in Table3. As can be seen, the RSD values of the measurements were not greater than 1.89% and 2.10% intra-day and inter-day determination, respectively and the value of recovery is ranged from 97.5% to 102.5%. Both the intra-day and inter-day reproducibilities of the voltammetric method were fairly good. The obtained results confirm the good precision and accuracy for determination of CPX by SWV method using the fabricated Au-In_2O_3-CS/ABPE.

Table3 Here

The robustness of the proposed procedure (TableS1) was also examined by studying the effect of small variations in pH, E_{acc} and t_{acc} on the recovery of CPX .As can be seen from TableS1, % R was in the range of 97.74–102.45% under all variable conditions and did not show any significant change when the critical parameters were varied which implies that the method is robust in nature.

3.12. Selectivity

In order to evaluate the selectivity of the proposed sensor for the determination of CPX, the influence of potentially interfering substances such as ascorbic acid, uric acid, dopamine, alanine, phenylalanine, uracil, cysteine, glucose, citric acid, cytosine, histidine, serine and mannitol was investigated. Tolerance limit was defined as the maximum concentration of the potential interfering substance that caused an error less than ±5% for the determination of CPX. Under the optimum conditions, the electrochemical response of 1.38 μmol L^{-1} CPX was detected in the presence of different concentrations of foreign species (TableS2). As shown in TableS2, the results showed that 250-fold of ascorbic acid and cysteine, 200-fold of uric acid, uracil and histidine, 300-fold of alanine, phenylalanine, citric acid and serine, 150-fold dopamine, 500-fold glucose and 100-fold cysteine did not interfere the detection with the peak current change less than ±5%. The results obtained show also recoveries in the range from 97.23% to 101.89% indicating that there were no important matrix interferences for the samples by the proposed SWV method using Au-In_2O_3-CS/ABPE. The interference analysis depicts high selectivity of the Au-In_2O_3-CS/ABPE sensor for the determination of CPX. The selectivity of the developed sensor is likely due to the synergistic effect of Au-In_2O_3-CS nanobiocomposite which provided better electron transfer efficiency between CPX and the working electrode and increased the catalytically active surface of the Au-In_2O_3-CS nanobiocomposite. From these results, it may be concluded that the method is free from interference by most coexisting substances and shows promising properties for use in real samples.

3.13. Analytical applications

3.13.1. Determination of CPX in Batrafen cream

In view of the above results, the applicability of the prepared modified electrode was tested by determination of the content of CPX in cream as a real pharmaceutical sample using SWV. It was

found that the pursuing the proposed method, the recovery test was carried out by adding a known amount of CPX standard into the sample (Fig.11). The obtained results obviously show that cream matrix does not have any interference effect on the electrochemical analysis of CPX. The accuracy of the proposed method was studied by evaluation of recoveries in three level concentrations of the spiked CPX to the cream samples. The accuracy and precision of the proposed SWV using modified electrode Au-In_2O_3-CS/ABPE for assay CPX in investigated cream samples were examined (Table4). The value of recovery is in the range from 98.26 % to 99.42% indicating the proposed sensor in this work is efficient for CPX determination in real samples with high sensitivity and precision. For comparison, the samples were also determined with a reference method of ultra performance liquid chromatography (UPLC). For UPLC analysis, a calibration graph was prepared by plotting CPX concentration versus peak area (Fig.S9). As shown in Table 4, the results obtained by this proposed method were in good agreement with those obtained by UPLC method. Applying a paired F- and t-tests on the results obtained by the proposed procedure and those obtained by the UPLC method, it was found that all results are in agreement at the 95% confidence level. The experimentally calculated values of F- and t-tests were less than that of theoretical values for F- (19) and t-(2.13) tests (Table4).

Figure11 Here

Table4 Here

3.13.2. Determination of CPX in Batrafen solution (ear drops)

The practical applicability of the optimized sensor was also investigated by detecting CPX in ear drops samples. Prior to measurements, the Batrafen solution samples were diluted using MB of pH 4.0. SWVs were recorded after addition of the standard CPX solution in potential range of +0.3 V to 1.1 V. Typical standard additions curves for CPX are shown in Fig.12. The observed increase in the peak current after the addition of CPX to Batrafen sample clearly indicated that the observed peak at 0.84V for Batrafen sample corresponds to the oxidation of CPX. The obtained results for different Batrafen samples are shown in Table4. As can be seen, the recovery results of different amounts of CPX in Batrafen are varying in the range 97.39 % to 99.62 % with a less relative standard deviation (RSD), indicating the determination procedures are free from interferences of the Batrafen sample matrix. These results showed that the proposed sensor was very satisfactory in determination of CPX in real

samples. The proposed method was further validated by employing UPLC (Table 4). This Table shows that the amount of CPX obtained by the proposed method agreed well with the amount obtained by the UPLC method. The obtained results demonstrated that the modified electrode has satisfactory analytical performance and can be a feasible sensor for determination of CPX in real samples.

Figure12 Here

4. Conclusion

Novel nanobiocomposite which consists of Au decorated In_2O_3 nanoparticles and chitosan was successfully prepared and used for modification of acetylene black paste electrode. The chitosan porous provided a large surface area for the entrapped nanocomposite of Au-In_2O_3 and facilitated the analyte's access to the sensing material. The combined electrocatalytic and synergistic properties of Au-In_2O_3 and the large surface area of CS showed a significant improvement in electrical conductivity as mentioned from the cyclic voltammetry of the redox couple $[Fe(CN)_6]^{3-/4-}$. The different percentages of each CS and Au-In_2O_3 nanocomposites incorporated acetylene black paste electrode revealed a significant influence on the voltammetric response of the modified electrode and evident change in surface area. The surface of Au-In_2O_3-CS nanobiocomposite modified ABPE showed an excellent electrocatalytic performance in the detection of antimycotic CPX and offered higher sensitivity compared to unmodified ABPE. The detection limit of CPX at this biosensor using SWV mode was 6.64×10^{-9} mol L^{-1}. Moreover, the Au-In_2O_3-CS/ABPE performed well in the detection of CPX in Batrafen cream and ear drops as real pharmaceutical samples. The developed biosensor provides a new avenue for electrochemical investigation of CPX for potential use in pharmaceutical and clinical preparations.

References

[1] S. Shahrokhian, M. Ghalkhani, Electrochemical study of Azathioprine at thin carbon nanoparticle composite film electrode, Electrochem. Commun. 11 (2009) 1425-1428.

[2] S. Peng, L. Tian, J. Liang, S.G. Mhaisalkar, S. Ramakrishna, Polypyrrole nanorod networks/carbon nanoparticles composite counter electrodes for high-efficiency dye-sensitized solar cells, ACS Appl. Mater. Interfaces 4 (2012) 397-404.

[3] D.I. Bower, An introduction to polymer physics, Cambridge University Press (2002).

[4] Y.C. Tsai, S.C. Li, S.W. Liao, Electrodeposition of polypyrrole–multiwalled carbon nanotube–glucose oxidase nanobiocomposite film for the detection of glucose, Biosensors and Bioelectronics 22 (2006) 495-500.

[5] L.T. Ma, H.Q. Fan, H.L. Tian, J.W. Fang, X.Z. Qian, The n-ZnO/n-In_2O_3 heterojunction formed by a surface-modification and their potential barrier-control in methanal gas sensing, Sens. Actuators B 222 (2016) 508–516.

[6] P. Li, H.Q. Fan, Y. Cai, M.M. Xu, Zn-doped In_2O_3 hollow spheres: mild solution reaction synthesis and enhanced Cl_2 sensing performance, Cryst. Eng. Comm. 16 (2014) 2715–2722.

[7] H.X. Bai, L.X. Zhang, Y.C. Zhang, Simple synthesis of urchin-like In_2S_3 and In_2O_3 nanostructures, Mater. Lett. 63 (2009) 823-825.

[8] H. Ibrahim, Y. Temerk, Novel sensor for sensitive electrochemical determination of luteolin based on In_2O_3 nanoparticles modified glassy carbon paste electrode, Sens. Actuators B: Chemical 206 (2015) 744-752.

[9] S. Shahrokhian, M. Ghalkhani, Glassy carbon electrodes modified with a film of nanodiamond–graphite/chitosan: Application to the highly sensitive electrochemical determination of azathioprine, Electrochim. Acta 55 (2010) 3621-3627.

[10] J. Ma, Y. Sahai, Chitosan biopolymer for fuel cell applications, Carbohydrate Polymers 92 (2013) 955-975.

[11] F. Belliardo, A. Bertolini, G. Brandolo, C. Lucarelli, Micro-liquid chromatography method for the determination of ciclopiroxolamine after pre-column derivatization in topical formulations, J. Chromatogr.A 553 (1991) 41-45.

[12] T.C. Ma, B. Langley, B. Ko, A screen for inducers of p21(waf1/cip1) identifies HIF prolylhydroxylase inhibitors as neuroprotective agents with antitumor properties, Neurobiol Dis. 49C (2012) 13–21.

[13] S. Song, T. Christova, S. Perusini, Wnt inhibitor screen reveals iron dependence of beta-catenin signaling in cancers, Cancer Res. 71 (2011) 7628–7639.

[14] Y. Eberhard, S.P. McDermott, X. Wang, Chelation of intracellular iron with the antifungal agent ciclopirox olamine induces cell death in leukemia and myeloma cells, Blood 114 (2009) 3064–3073.

[15] The United States Pharmacopeia and the National Formulary, USP 28, NF 23, United States Pharmacopoeia Convention Inc., Rockville, MD, 2005.

[16] The United States Pharmacopeia and the National Formulary, USP 25, NF 20, United States Pharmacopoeia Convention Inc., Rockville, MD, 2002.

[17]] F. Nacaratte, M.I. Toral, C. Soto, Development of a kinetic spectrophotometric method for the determination of ciclopirox olamine in pharmaceutical sample, J. Chil. Chem. Soc. 61 (2016) 3102-3107.

[18] A.L.V. Escarrone, C.F. Bittencourt, L.V. Laporta, M.R. dos Santos, E.G. Primel, S.S. Caldas, LC-UV method with pre-column derivatization for the determination of ciclopirox olamine in raw material and topical solution, Chromatographia 67 (2008) 967-971.

[19] M.I. Walash, M.S. Rizk, M.I. Eid, M. Fathy, E. Sayed, Spectrofluorimetric determination of ciclopirox olamine via ternary complex with Tb(III) and EDTA Acta Pharma. 56 (2006) 431-440.

[20] L.M.C. Ferreira, F.S. Felix, L. Angnes, Fast determination of ciclopirox in pharmaceutical products by amperometry in flow and batch injection systems, Electroanalysis 24 (2012) 961-966.

[21] A.P.R. Souza, F.S. Felix, P.S. Castro, L. Angnes, M. Bertotti, Gold random microarrays: design, characterization and amperometric determination of ciclopirox olamine in pharmaceutical products, Anal. Methods 8 (2016) 1078-1083.

[22] F. Ibrahim, N. El-Enany, Anodic polarographic determination of ciclopirox olamine in pure and certain pharmaceutical preparations, J. Pharm. Biomed. Anal. 32 (2003) 353-359.

[23] F. Ibrahim, N. El-Enany, Polarographic determination of ciclopirox olamine in pure substance and in different pharmaceutical preparations, II Farmaco 58 (2003) 1313-1318.

[24] K.M. Lukasiewicz, K. Roginska, Voltammetric determination of antifungal agents in pharmaceuticals and cosmetics using boron-doped diamond electrodes, Anal. Methods 6 (2014) 7912–7922.

[25] J. Li, Y. Jiang, T. Sun, S. Ren, Fast and simple method for assay of ciclopirox olamine by micellar electrokinetic capillary chromatography, J. Pharm. Biomed. Anal. 47 (2008) 929-933.

[26] W. Bu, X. Fan, H. Sexton, I. Heyman, A direct LC/MS/MS method for the determination of ciclopirox penetration across human nail plate in in vitro penetration studies, J. Pharm. Biomed. Anal. 51 (2010) 230-235.

[27] F.S. Felix, C.L.L. Angnes, Determination of ciclopirox olamine in pharmaceutical products by capillary electrophoresis with capacitively coupled contactless conductivity detection, Electrophoresis 32 (2011) 900-905.

[28] C. Soto, R. Saavedra, M.I. Toral, F. Nacaratte, C. Poza, Preliminary studies for ciclopirox olamine determination by thermal lens spectrophotometry, Microchemical J. 129 (2016) 36–40.

[29] R.J. Reay, A.F. Flannery, C.W. Storment, S.P. Kounaves, G.T. Kovacs, Microfabricated electrochemical analysis system for heavy metal detection, Sens. Actuators, B: Chem. 34 (1996) 450–455.

[30] X. Lu, Z. Wen, J. Li, Hydroxyl-containing antimony oxide bromide nanorods combined with chitosan for biosensors, Biomaterials 27 (2006) 5740–5747.

[31] Y. Wang, J. Lu, L. Tang, H. Chang, J. Li, Graphene oxide amplified electrogenerated chemiluminescence of quantum dots and its selective sensing for glutathione from thiol-containing compounds, Anal. Chem. 81 (2009) 9710–9715.

[32] M. Wang, C. Sun, L. Wang, X. Ji, Y. Bai, T. Li, J. Li, Electrochemical detection of DNA immobilized on gold colloid particles modified self-assembled monolayer electrode with silver nanoparticle label, J. Pharm. Biomed. Anal. 33 (2003) 1117–1125.

[33] B.D. Cullity, Elements of X-ray Diffraction, 2nd ednR, Addison Wesley, Reading, MA, 1978.

[34] R.N. Goyal, V.K. Gupta, S. Chatterjee, Voltammetric biosensors for the determination of paracetamol at carbon nanotube modified pyrolytic graphite electrode, Sens. Actuators B: Chem. 149 (2010) 252–258.

[35] D.K. Gosser, Cyclic voltammetry: simulation and analysis of reaction mechanisms, VCH, New York (1993).

[36] E. Laviron, General expression of the linear potential sweep voltammogram in the case of diffusionless electrochemical systems, J. Electroanal. Chem. 101 (1979) 19-28.

[37] E. Laviron, The use of linear potential sweep voltammetry and of a.c. voltammetry for the study of the surface electrochemical reaction of strongly adsorbed systems and of redox modified electrodes, J. Electroanal. Chem. 100 (1979) 263-270.

[38] Y.M. Temerk, P. Valenta, H.W. Nūrnberg, Voltammetric studies on the adsorption and association of the oligonucleotide cytidylyl-(3 → 5)-cytidine at the mercury-solution interface, J. Electroanal. Chem. 131(1982) 265-277.

Figures Legends:

Scheme1: Molecular structure of ciclopirox olamine (CPX).

Scheme 2. Schematic diagram of the CPX detection at ABPE and at the Au-In_2O_3-CS/ABPE.

Fig.1: XRD patterns of pure In_2O_3 and Au-In_2O_3 nanocomposite, Inset SAED of In_2O_3.

Fig.2: High-resolution TEM images of In_2O_3 (A), the Au-In_2O_3 nanocomposite (B&C) and lattice fringes image of Au-In_2O_3 nanocomposite (D).

Fig.3: SEM images of ABPE (A), In_2O_3/ABPE (B) Au-In_2O_3/ABPE (C) and Au-In_2O_3-CS/ABPE (D).

Fig.4: Cyclic voltammograms of 5 mmol L^{-1} $[Fe(CN)_6]^{-3/-4}$ in 0.1 mol L^{-1} KCl obtained at a scan rate of 100 mV/s. (a) bare ABPE, (b) CS/ABPE, (c) In_2O_3NPs/ABPE, (d) Au-In_2O_3/ABPE and (e) Au-In_2O_3-CS/ABPE**.**

Fig.5: (A) CVs at bare ABPE (1), CS/ABPE (2), In_2O_3/ABPE (3), Au-In_2O_3/ABPE (4) and Au-In_2O_3-CS/ABPE (5) in MB (pH 4.0) containing 7.41µmol L^{-1} CPX, scan rate, 100 mV s^{-1}. (B) SWVs at bare ABPE (1), CS/ABPE (2), In_2O_3/ABPE (3), Au-In_2O_3/ABPE (4) and Au-In_2O_3-CS/ABPE (5) in MB (pH 4.0) containing 4.03 µmol L^{-1} CPX, f = 100 Hz, ΔE_a = 30 mVpp and ΔE_s = 8 mV.

Fig.6: SW voltammograms of 4.03 µmol L^{-1} CPX at electrodes fabricated from 100 µL CS/ABPE modified with different percentage of Au-In_2O_3 nanocomposite (1) 0, (2) 2.5, (3) 5, (4) 7, (5) 10, (6) 12 and (7) 15%. Inset: the peak current of CPX as a function Au-In_2O_3 nanocomposite content.

Fig.7: The peak current of CPX as a function CS volume.

Fig.8: Effect of pH on E_P(●) and I_P(▲) for CPX.

Fig.9: (A) CVs of 7.41 µmol L^{-1} CPX on the surface of Au-In_2O_3-CS/ABPE at various scan rates in MB (pH4.0); (1) 50, (2) 100, (3)150, (4)200, (5) 250, (6) 300, (7) 350, (8) 400, (9) 450 and (10) 500 mVs^{-1}. (B) Plot of peak current (I_{pa}) versus square root of scan rate ($\nu^{1/2}$). (C) Plot of log of peak current (log I_{pa}) versus log of scan rate (log ν).

Fig.10: SWVs of different concentrations of CPX in MB of pH 4.0 at Au-In_2O_3-CS/ABPE: (1) 0.0, (2) 0.199, (3) 0.398, (4) 0.596, (5) 0.794, (6) 0.99, (7) 1.18, (8) 1.38, (9) 1.77, (10) 2.15, (11) 2.53, (12) 3.29, (13) 4.03, (14) 4.94, (15) 5.84, (16) 7.1, (17) 8.01, (18) 9.23, (19) 10.27, (20) 12.57 and (21) 16.22 µmol L^{-1} CPX. E_{acc}, +0.1 V; t_{acc}, 70s; scan increment, 8 mV; frequency, 100 Hz and pulse height, 30 mV.

Fig.11: SW voltammograms for determination of CPX in Batrafen cream sample in MB of pH4.0 at Au-In_2O_3-CS/ABPE. 1) Batrafen sample, 2) (1) + 1.18 µmol L^{-1}, 3) (1) +1.57 µmol L^{-1}, 4) (1) + 2.15 µmol L^{-1}, 5) (1) + 2.91 µmol L^{-1}, 6) (1) + 3.85 µmol L^{-1}, 7) (1) +4.94 µmol L^{-1}, 8) (1) + 6.19 µmol L^{-1}, 9) (1) + 7.57 µmol L^{-1}, 10) (1) + 8.75 µmol L^{-1} and 11) 1+ 9.91 µmol L^{-1} CPX.

Fig.12: SW voltammograms for determination of CPX in Batrafen solution sample in MB of pH4.0 at Au-In_2O_3-CS/ABPE. 1) Batrafen solution sample, 2) (1) + 1.18 µmol L^{-1}, 3) (1) +1.57 µmol L^{-1}, 4) (1) + 2.15 µmol L^{-1}, 5) (1) + 2.91 µmol L^{-1}, 6) (1) + 3.70 µmol L^{-1}, 7) (1) +4.58 µmol L^{-1}, 8) (1) + 6.01 µmol L^{-1}, 9) (1) + 7.75 µmol L^{-1} and 10) (1) + 9.05 µmol L^{-1} CPX.

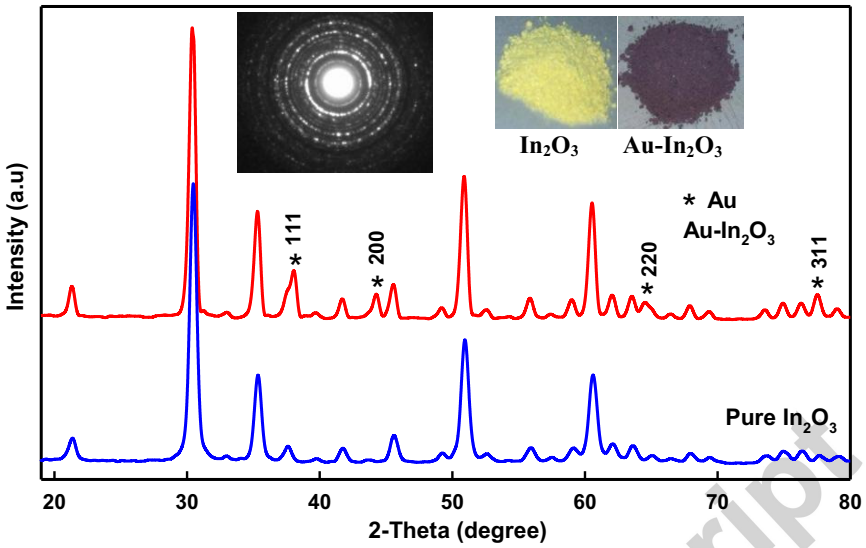

Fig.1:

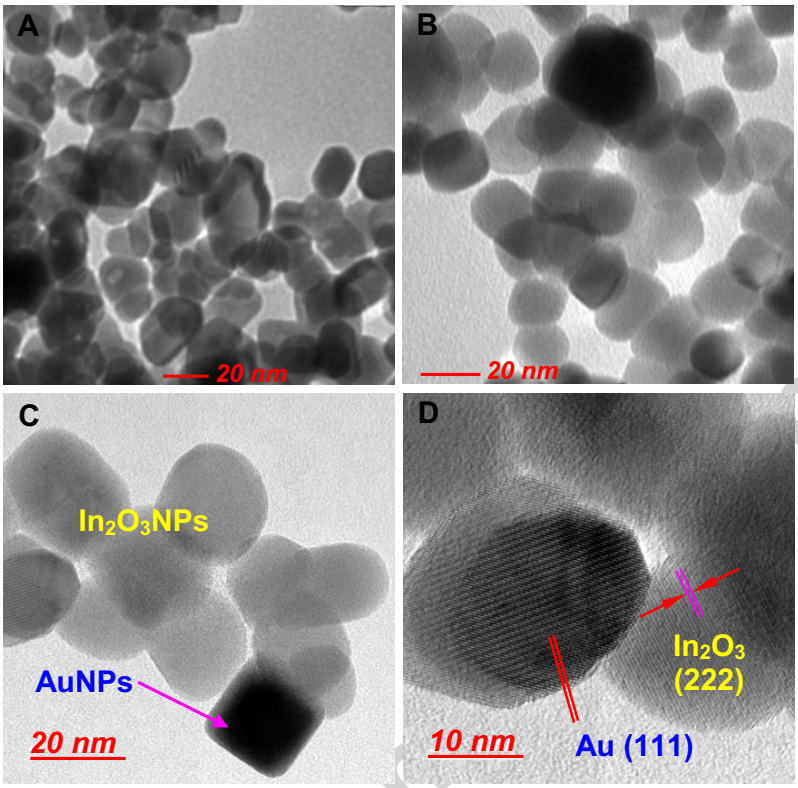

Fig.2:

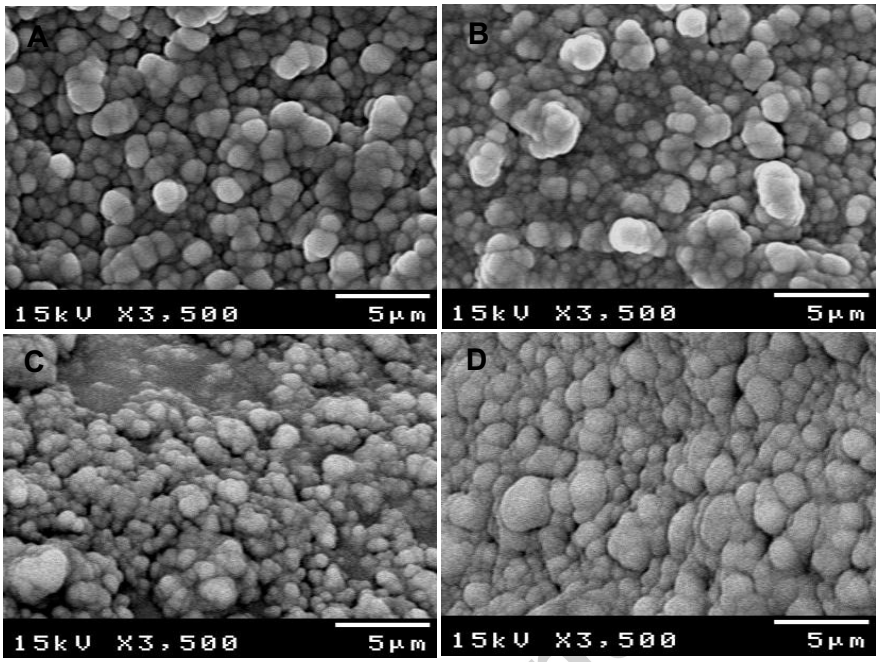

Fig.3:

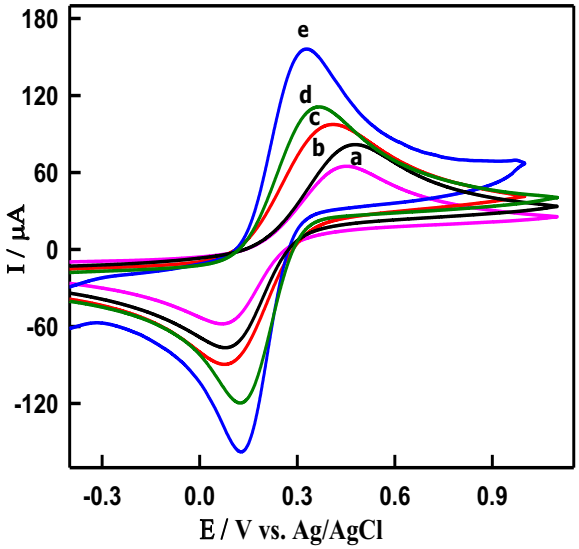

Fig.4:

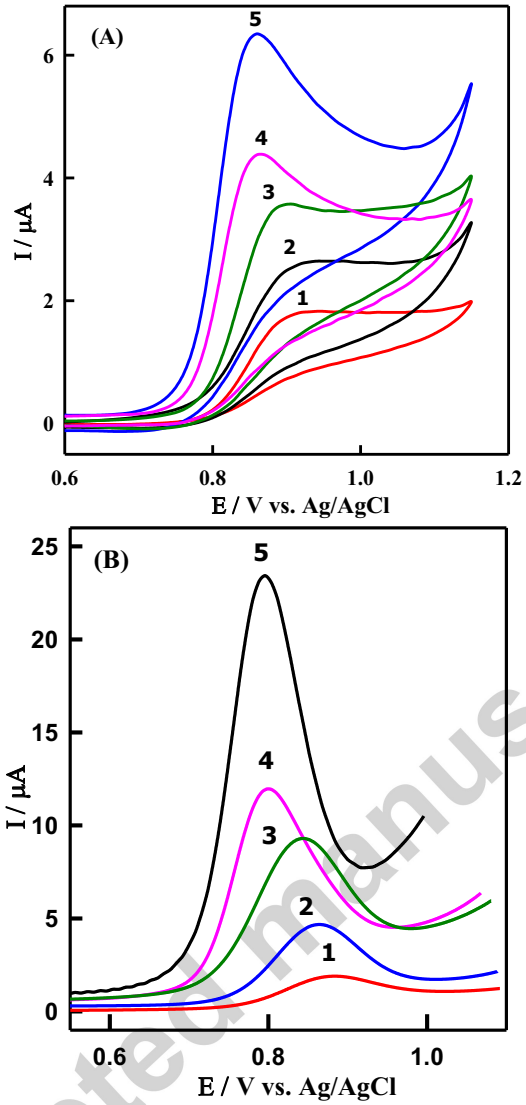

Fig.5:

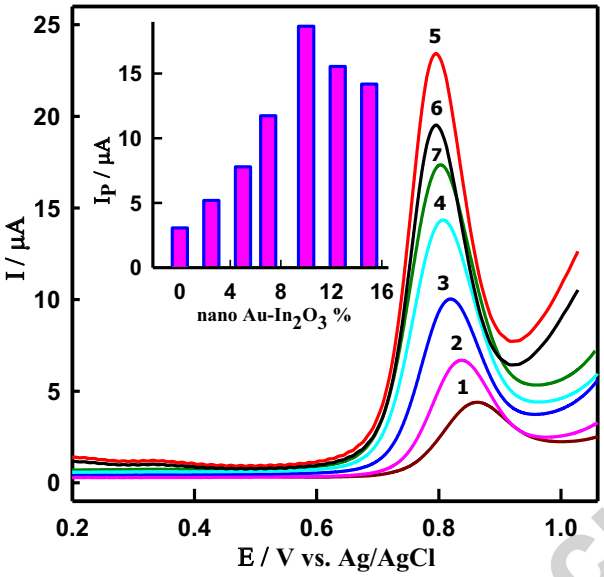

Fig.6:

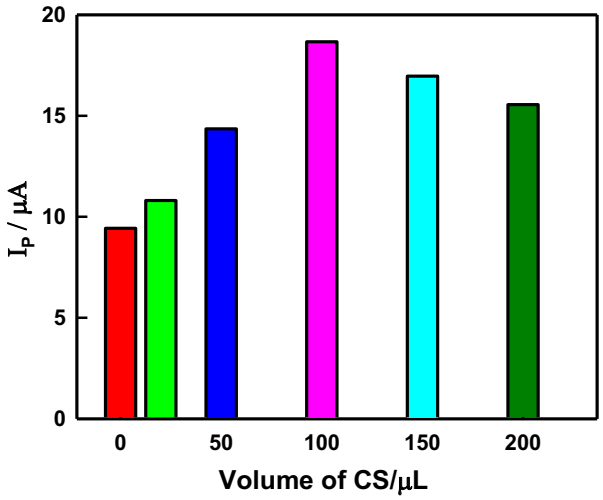

Fig.7:

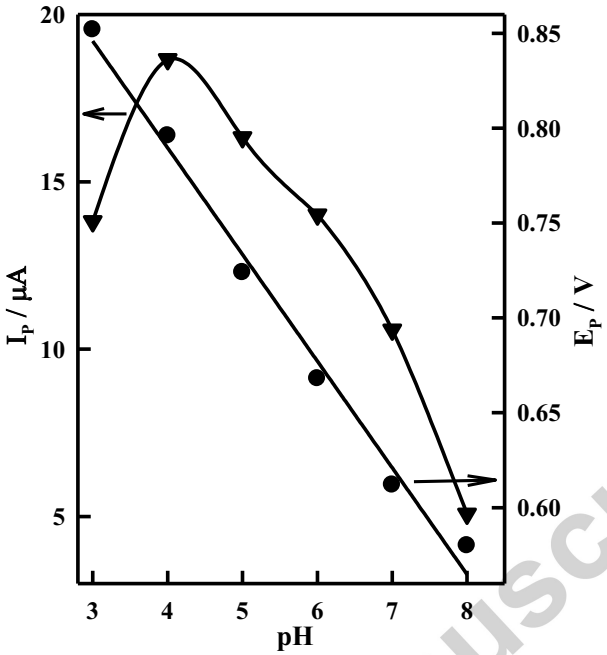

Fig.8:

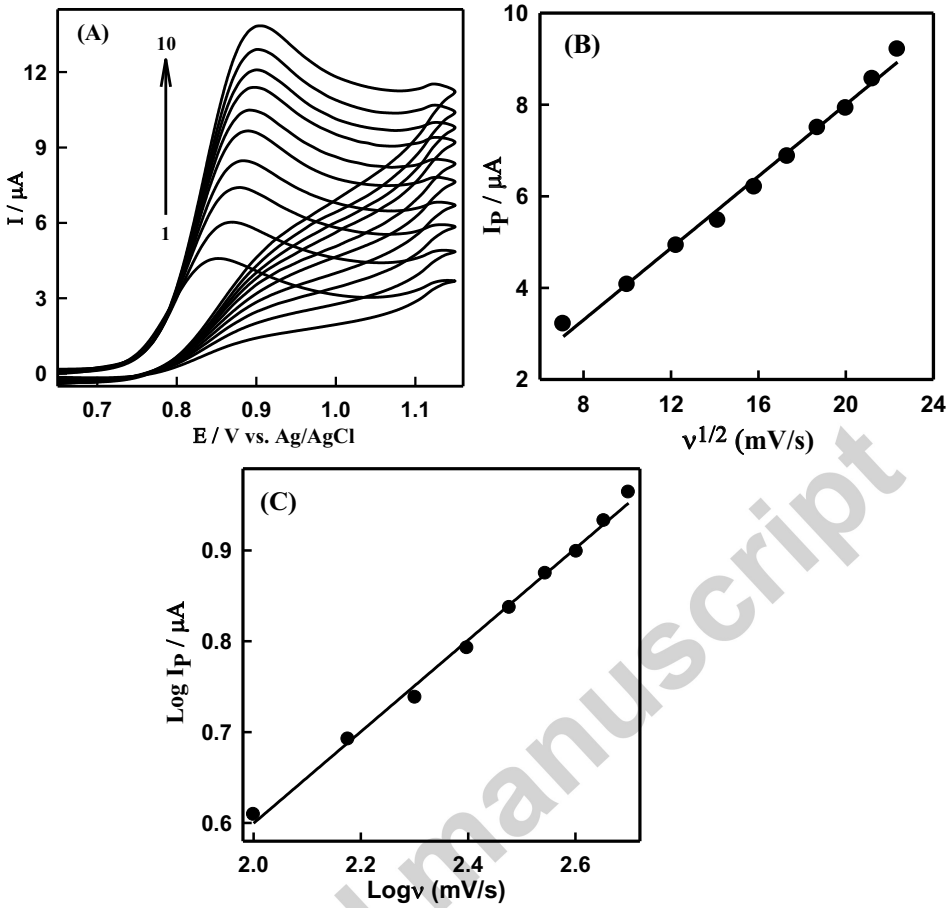

Fig.9:

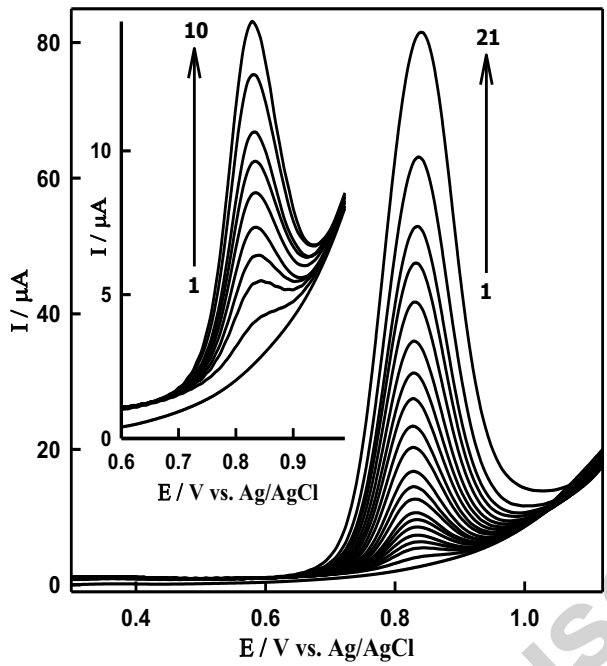

Fig.10:

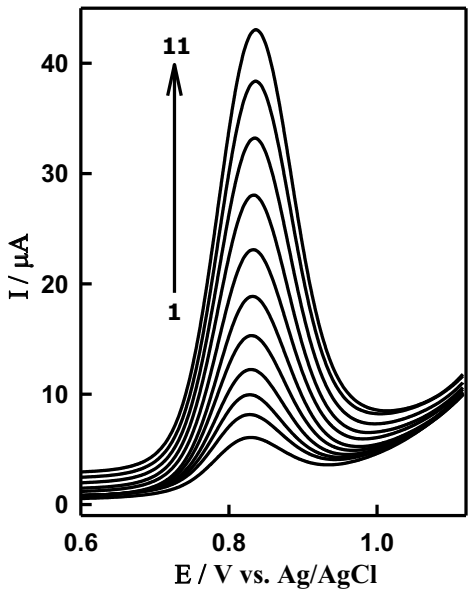

Fig.11:

Figure12

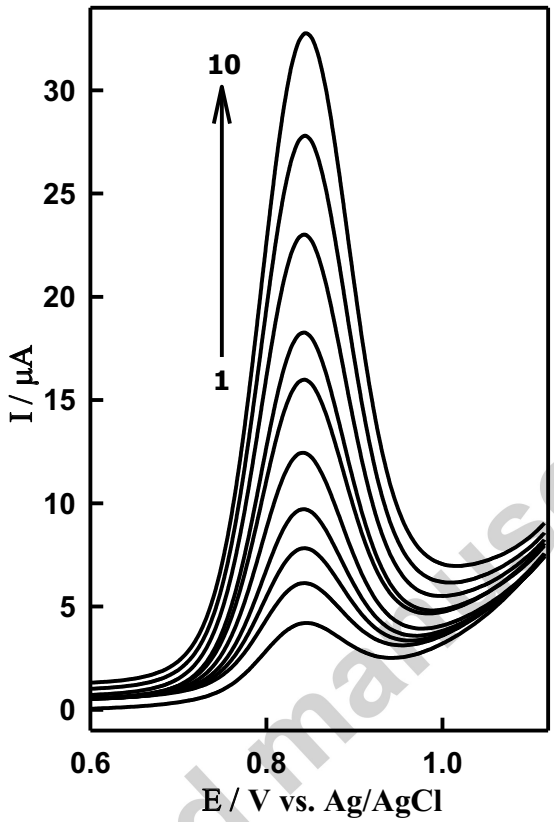

Fig.12:

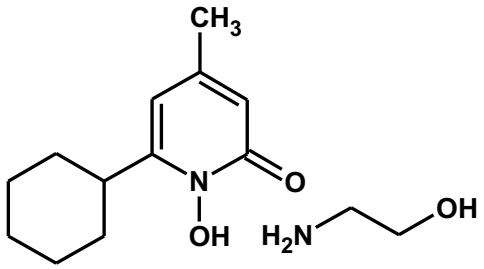

Scheme1:

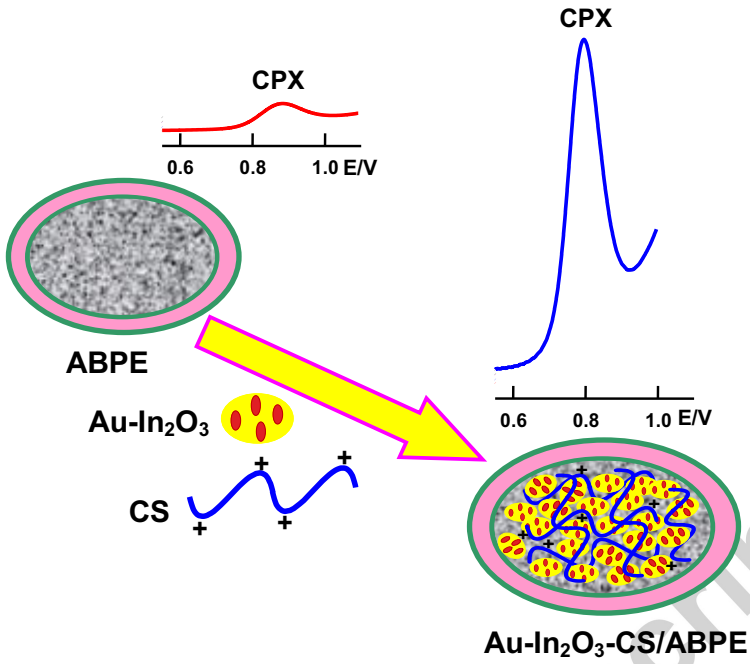

Scheme 2.

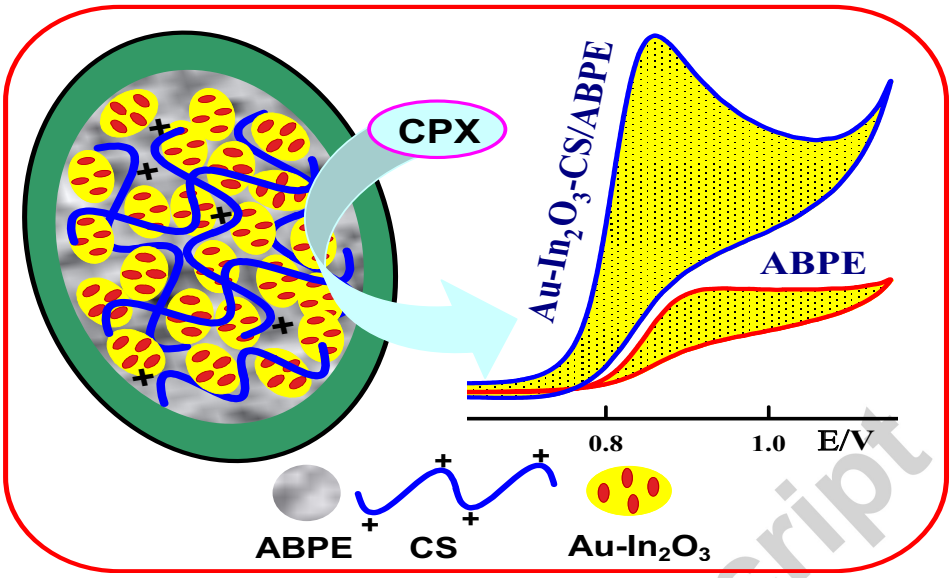

Novel nanobiocomposite which consists of Au decorated In_2O_3 nanoparticles and chitosan was successfully prepared and used for modification of acetylene black paste electrode. The chitosan porous provided a large surface area for the entrapped nanocomposite of Au-In_2O_3 and facilitated the analyte's access to the sensing material. The analytical performance of this biosensor was evaluated for detection of CPX in pharmaceutical formulations with good accuracy and precision.

Table 1: Regression data of the calibration lines for quantitative determination of CPX in McIlvaine's buffer (pH 4.0) at Au–In_2O_3-CS/ABPE using SWV

Parameters	Standard solution
Working electrode potential (V)	0.835
Linearity range (μM)	0.199 – 16.22
Slope (μAM^{-1})	4.52×10^6
SE of slope	0.026
Intercept (μA)	0.04
SE of intercept	0.17
Determination coefficient (R^2)	0.9994
Number of data points	20
LOD (M)	6.64×10^{-9}
Sensitivity ($\mu A\ \mu M^{-1}\ cm^{-2}$)	64.57
Repeatability of peak current (RSD%)	0.86
Reproducibility of peak current (RSD%)	0.79

Table 2: Some analytical methods for the determination of CPX

Method	Linearity range (μM)	LOD (M)	Ref.
Spectrophotometric	1.54 – 480	4.58×10^{-7}	17
Chromatography	1 – 100	4.0×10^{-8}	18
Amperometry	2.0 – 200	1.0×10^{-6}	20
Amperometry	60 – 1100	3.0×10^{-6}	21
Anodic polarography	9 – 58	9.0×10^{-7}	22
SWV	25.3 – 419	6.66×10^{-6}	24
MEKC	149 – 647	4.51×10^{-5}	25
LC/MS	0.038 – 1.23	1.15×10^{-8}	26
CE	12.7 – 1270	1.88×10^{-6}	27
SWV	0.199 – 16.22	6.64×10^{-9}	This work

(MEKC) Micellar Electrokinetic Capillary Chromatography, (LC-MS) Liquid Chromatography–Mass Spectrometry, (CE) Capillary Electrophoresis,

Table 3: Precision (Intra and Inter day) and accuracy for assay of CPX (n=5)

Added (μM)	Found (μM)	Precision RSD %	Relative error %	Recovery %
		Intra-day		
0.40	0.41 ± 0.014	1.72	-2.44	102.5
1.77	1.74 ± 0.018	1.39	1.69	98.30
7.10	7.06 ± 0.021	1.89	0.56	99.43
		Inter-day		
0.40	0.39 ± 0.012	2.10	2.50	97.5
1.77	1.75 ± 0.024	1.78	1.13	98.87
7.10	7.13 ± 0.041	1.58	-0.42	100.42

Table 4: Results of CPX determination in real samples by SWV compared with UPLC method

Pharmaceutical preparation	Proposed method (n=3)			UPLC method (n=3)		*F-test*	*t-Test*
	Added ($\mu mol\ L^{-1}$)	Found ($\mu mol\ L^{-1}$)	Recovery (%)	Found ($\mu mol\ L^{-1}$)	Recovery (%)		
Batrafen solution (10 mg of CPX per mL)	1.15	1.13	98.26	1.11	96.52	1.048	0.140
	3.20	3.16	98.75	3.14	98.12	1.140	0.210
	5.25	5.22	99.42	5.29	100.76	1.058	0.182
Mean ± SD			98.81±0.58		98.47±2.14		
Batrafen cream (10 mg of CPX per g)	1.15	1.12	97.39	1.10	95.65	1.027	0.231
	3.20	3.14	98.13	3.12	97.50	1.210	0.173
	5.25	5.23	99.62	5.18	98.70	1.180	0.187
Mean ± SD			98.38±1.13		97.28±1.45		

Theoretical F-value 19 and t-test value = 2.13 at 95% confidence limit for $n_1 = 3$ and $n_2 = 3$

- A novel nanobiocomposite sensor based on Au-In_2O_3-CS/ABPE was developed
- The Au-In_2O_3-CS/ABPE displays good biocompatibility, conductivity, and stability
- The bioelectrode showed electrocatalytic activity toward oxidation of CPX
- Analytical application of the electrodes was successfully applied for detection of CPX in real samples